A unified approach for computing tsunami, waves, floods, and landslides

Alexander Danilov[1], Kirill Nikitin[1], Maxim Olshanskii[2], Kirill Terekhov[1], and Yuri Vassilevski[1]

[1] Institute of Numerical Mathematics RAS, Gubkin str. 8, 119333, Moscow, Russia a.a.danilov@gmail.com, nikitin.kira@gmail.com, kirill.terehov@gmail.com, yuri.vassilevski@gmail.com

[2] Department of Mathematics, University of Houston, Houston, Texas 77204-3008 molshan@math.uh.edu

Abstract. The prediction of large-scale hydrodynamic events such as tsunami spread and run-up, dam break, flood, or landslide run-out is a challenging and important problem of applied mathematics and scientific computing. The paper presents a computational approach based on free surface flow models for fluids of complex rheology to simulate such events and phenomena with detail and prediction confidence typically not achievable by simplified models. Using nonlinear defining relations for stress and rate of strain tensors allows a unified approach to simulate events described by both the Newtonian model (tsunami, dam break) and non-Newtonian models (landslide, snow avalanches, lava flood, mud flow). The computational efficiency of the numerical approach owes to the level-set method for free surface capturing and to an accurate and stable FV/FD method on dynamically adapted octree meshes for discretization of flow and level set equations. In this paper we briefly describe the numerical method and present results of several simulations of hydrodynamic events: a dam break, a landslide and tsunami spread and run-up.

1 Introduction

Numerical simulations became a standard tool for the study and prediction of disasters and events involving water and mud flows, landslides, avalanches and other phenomena described by equations of continuous medium. Since the computational complexity of full-scale simulations of such events is highly demanding for computer resources, it is common to describe phenomena by reduced-order approaches, for example, based on 2D and even 1D equations and simplified rheological models. A few examples are the use of the shallow water equations [13,18] to simulate the spread of tsunami or modified hydrodynamics equations to compute landslide and debris flows [4].

In this paper, we describe a computational approach that allows one to simulate many of complex hydrodynamic events using fewer simplifying assumptions to describe the physics of flows and accounting for their three-dimensional nature and real environment. Instead of models based on shallow water theory or other approaches using simplified physics, we use the full

system of incompressible Navier-Stokes equations for flows with free surface. The necessary model order reduction is then happen on the numerical method stage of simulations and is essentially due to the use of accurate discretization schemes on dynamically adapted octree meshes. The phenomenological diversity of the processes we are interested in is accounted by the choice of proper nonlinear relations between the stress and the strain rate tensors. We consider both Newtonian model to describe dam break and ocean tsunami flows and visco-plastic Hershel-Bulkley model for landslides. However, the developed numerical technology makes it easy for a researcher to incorporate different, even more complicated, defining relations.

In all flows considered here, finding free surface dynamics is critical. To capture the free surface evolution, we apply the level set method [15]. We discretize flow and level set equations using octree meshes. Discretizations on octree meshes benefit from their regular orthogonal structure on one hand and the embedded hierarchy on the other hand, which make the reconstruction and adaptation process as well as data access fast and easy. Nowadays such grids are widely used in simulations and visualization, see, e.g., [5,7,8,10,14,17]. However, building accurate and stable discretizations on such grids is a challenging task. For the fluid equations we use the second order accurate finite difference/finite volume method with compact nodal stencils developed in [11]. This method is a stable extension of the classical MAC scheme on octree meshes. Semi-Lagrangian particle level set method [12] is used to solve the transport equation for the level set function. To integrate in time, we apply a second order splitting scheme of Chorin type. This scheme decouples one time step on convection, diffusion and plasticity, pressure correction, and the level set function advection substeps. Numerical stability and accuracy of the whole method were verified for the case of Newtonian flows in [9,11] by computing analytical solutions and benchmark flows in a cubic cavity and over a 3D cylinder. Computed results for a collapsing water column perfectly match available experimental data. The efficiency of the approach for non-Newtonian flows was accessed in [10,17], where the flow of Hershel-Bulkley fluid from a reservoir over inclined planes was computed and compared to documented experimental results with Carbopol Ultrez 10 gel. These results let us believe that the entire approach is computationally efficient, highly predictive and so is the reliable tool for simulation of large-scale hydrodynamic events.

The remainder of the paper is organized as follows. The mathematical model is given in section 2. In section 3, we sketch the basics of the numerical approach. In section 4, we discuss our approach to the topography-specific design of the computational domain. Section 5 presents results of numerical simulations of three hypothetical scenarios: the break of the Sayano-Shushenskaya dam, landslide in the Sayan mountains and tsunami run-up in the Bay of Bengal. The computations were done using real topography and bathymetry. It is remarkable that such different natural disaster scenarios

can be simulated in a unified framework of computational non-Newtonian fluid dynamics.

2 Mathematical model

Conservation of mass and momentum for an incompressible viscous fluid leads to the Navier-Stokes equations for the unknown velocity field $\mathbf{u}$ and stress tensor $\boldsymbol{\tau}$:

$$\begin{cases} \rho\left(\dfrac{\partial \mathbf{u}}{\partial t} + (\mathbf{u}\cdot\nabla)\mathbf{u}\right) - \mathbf{div}\ \boldsymbol{\tau} = \mathbf{f} \\ \nabla\cdot\mathbf{u} = 0 \end{cases} \quad \text{in } \Omega(t), \tag{1}$$

where $\mathbf{f}$ are given mass forces, $\Omega(t) \in \mathbb{R}^3$ is a spatial domain occupied by fluid and dependent on time, ρ is the density. For the strain rate tensor $\mathbf{Du} = \frac{1}{2}[\nabla\mathbf{u} + (\nabla\mathbf{u})^T]$ and the stress tensor we consider the Hershel-Bulkley defining relations [3]:

$$\begin{aligned} \boldsymbol{\tau} = -p\,\mathbf{I} + \left(K\,|\mathbf{Du}|^{n-1} + \tau_s|\mathbf{Du}|^{-1}\right)\mathbf{Du} \ &\Leftrightarrow\ |\boldsymbol{\tau}| > \tau_s, \\ \mathbf{Du} = \mathbf{0} \ &\Leftrightarrow\ |\boldsymbol{\tau}| \le \tau_s, \end{aligned} \tag{2}$$

where K is the consistency parameter, τ_s is the yield stress parameter, n is the fluid index, p is the pressure. Newtonian flows correspond to the choice $\tau_s = 0$, $n = 1$. In computations we use a regularized model [10,17].

A volume occupied by fluid and the velocity field at $t = 0$ are assumed to be given:

$$\Omega(0) = \Omega_0, \quad \mathbf{u}|_{t=0} = \mathbf{u}_0. \tag{3}$$

Finding $\Omega(t)$ for $t > 0$ is a part of the problem which is solved together with equations (1). To formulate this more precisely, let us divide the boundary of the whole volume into the static boundary Γ_D (for instance, the rigid walls or the bottom of a bassin) and the free boundary $\Gamma(t)$ (in practice it usually models an interface between fluid and air), i.e. $\overline{\partial\Omega(t)} = \overline{\Gamma_D} \cup \overline{\Gamma(t)}$. Generally speaking, the static boundary Γ_D depends on time.

We assume the non-penetration condition on Γ_D and, depending on a physical setup, the no-slip or slip with friction conditions. The free boundary evolves with the normal velocity of fluid, which can be written as the kinematic condition

$$v_\Gamma = \mathbf{u}\cdot\mathbf{n}_\Gamma,$$

where $\mathbf{n}_\Gamma$ is the outer unit normal to the surface $\Gamma(t)$, v_Γ is the normal velocity of the surface $\Gamma(t)$. Normal stresses on the free surface are balanced by the surface tension forces. This leads to the boundary condition

$$\boldsymbol{\tau}\mathbf{n}_\Gamma = \varsigma\kappa\mathbf{n}_\Gamma - p_{\text{ext}}\mathbf{n}_\Gamma \quad \text{on } \Gamma(t), \tag{4}$$

where κ is the sum of the principal curvatures of the surface, ς is the surface tension coefficient, p_{ext} is the external pressure. If the surface tension forces are not taken into account, we may assume $\varsigma = 0$.

In order to find the position of the free boundary at each time moment we use instead of the kinematic condition the implicit definition of $\Gamma(t)$ as the zero level set of the globally defined indicator function $\phi(t, \mathbf{x})$:

$$\phi(t,\mathbf{x}) = \begin{cases} < 0 & \text{if } \mathbf{x} \in \Omega(t) \\ > 0 & \text{if } \mathbf{x} \in \mathbb{R}^3 \setminus \overline{\Omega(t)} \\ = 0 & \text{if } \mathbf{x} \in \Gamma(t) \end{cases} \qquad \text{for all } t \in [0,T].$$

The function ϕ is called the level set function. The level set function satisfies the following transport equation [12]:

$$\frac{\partial \phi}{\partial t} + \widetilde{\mathbf{u}} \cdot \nabla \phi = 0 \quad \text{in } \mathbb{R}^3 \times (0,T], \tag{5}$$

where $\widetilde{\mathbf{u}}$ is the fluid velocity field extended outside $\Omega(t)$. Initial condition (3) is used to define $\phi(0, \mathbf{x})$. one often imposes the additional restriction

$$|\nabla \phi| = 1 \tag{6}$$

onto the level set function to ensure numerical stability, i.e. ϕ is the signed distance function. Given ϕ, the outer normal and the curvature of the free boundary can be calculated from $\mathbf{n}_\Gamma = \nabla\phi/|\nabla\phi|$, $\kappa = \nabla \cdot \mathbf{n}_\Gamma$.

The mathematical model used in our calculations consists of equations (1), (2), (3), (4), (5), (6) and appropriate boundary conditions on static boundaries.

3 Numerical method

For the numerical time integration of (1)–(5) we use a second order splitting scheme of Chorin type with the BDF2 approximation of time derivative. For some given $\mathbf{u}(t)$, $p(t)$, $\phi(t)$ at time t, one time step consists in finding $\mathbf{u}(t+\Delta t)$, $p(t+\Delta t)$, $\phi(t+\Delta t)$, where Δt is a time increment. This is done in few substeps. First, using the second order semi-Lagrangian method [16], we integrate back in time the level set transport equation (5) along characteristics interpolated from previous time steps. At this step, one find the new volume occupied by a fluid, $\Omega(t) \to \Omega(t+\Delta t)$. Approximation errors may lead to a non-physical loss or gain of fluid volume, i.e. $|\Omega(t)| \neq |\Omega(t+\Delta t)|$ even in the absence of sources or sinks. To reduce this loss/gain of volume, we use the grid adaptation towards the free surface and the particle method [12]. This enhances the conservation properties of the semi-Lagrangian method significantly. If a further correction is still needed, one solves for δ the equation

$$\text{meas}\{\mathbf{x} : \phi(\mathbf{x}) \leq \delta\} = Vol^{\text{reference}}$$

and correct $\phi^{new} = \phi - \delta$. The above equation is solved for δ by the secant method for root finding and Monte-Carlo method to approximate meas$\{\mathbf{x}$:

$\phi(\mathbf{x}) < \delta\}$. For stability reasons, the substep is accomplished be the re-initialization of ϕ^{new} such that (6) holds, see [9,10]. After $\Omega(t+\Delta t)$ is found, we rebuild the octree mesh and re-interpolate all unknowns to the new mesh. If an extension of velocity (or pressure) to the exterior of $\Omega(t)$ is needed during the stages of re-interpolation or numerical integration of (5), then we perform the extension of unknowns along normals to free surface, i.e. the extension of velocity field satisfies $(\nabla\phi)\cdot\nabla\mathbf{u}(t) = 0$ in the exterior of $\Omega(t)$.

Further, one finds new values of hydrodynamic variables in $\Omega(t+\Delta t)$: $\{\mathbf{u}(t), p(t)\} \to \{\mathbf{u}(t+\Delta t), p(t+\Delta t)\}$. This is done in the following substeps: (i) The convective terms are approximated using the second order accurate compact upwind method on octree grids from [11] and the momentum equation is solved for an intermediate velocity, while the plasticity terms are treated explicitly [10]; (ii) The intermediate velocity field is projected onto the subspace of discrete divergence free functions and the pressure is updated by the solution of the discrete Poisson equation.

The time step is variable and controlled by a CFL type condition.

4 Design of computational domain

We use the Google SketchUp tool to generate a polygonal approximation of the earth surface and facilities on it in the area of interest. Depending on the problem the topographic data can be obtained from the Shuttle Radar Topography Mission (NASA), or the Google Maps, or the Google Earth projects. Ocean bathymetry can be retrieved from ETOPO data. As an example, the left picture of figure 1 shows the modeled 'broken' dam in a real life topography of Sayan mountains and Yenisei river. The scene of a rocky bay in the right picture is purely hand-made.

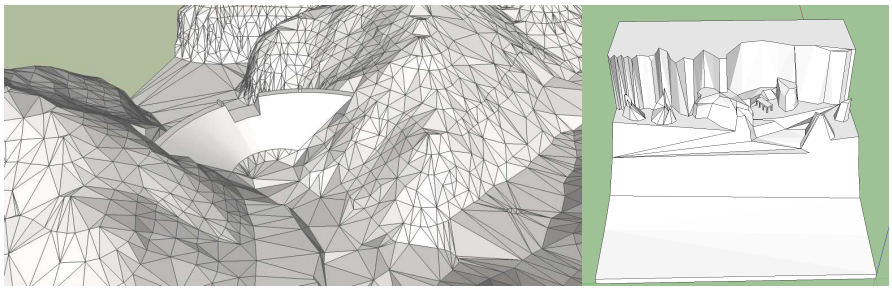

Fig. 1. Design of the computational domain using Google SketchUp software: environment of a dam (left), a rocky bay (right) .

5 Simulation of hydrodynamic events

In this section all variables are dimensional and given in the SI system.

First we present the results of simulations of the break of the Sayano-Shushenskaya dam. The calculations presented do not necessarily show any actual or feasible scenario for this hydro power plant. Rather, they show that with the present approach a prediction is practically possible, if more detailed geophysical data for the riverside area and the dam conditions are supplied. The computational domain and the part of the dam simulated as 'broken' are shown in green in figure 2 (left). The maximal number of active cells in the computational octree meshes was about 520 thousand. The water rise levels at given points are shown as graphs in figure 2 (right). The steplike graphs of the water level reflect the appearance of waves which are clearly seen on animation available from [19].

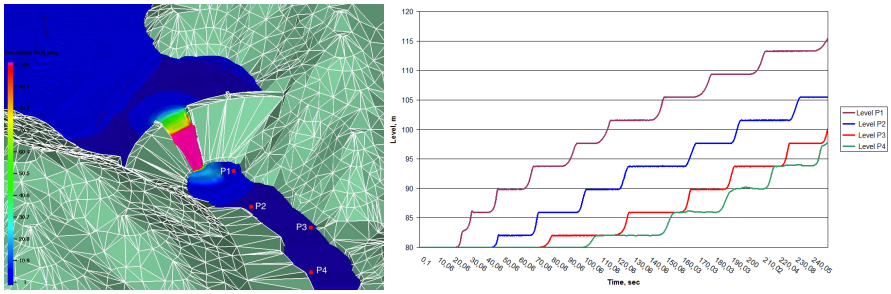

Fig. 2. Left: Mesh representation of the dam and the surrounding area. The monitoring of the water level variation is performed in the marked points. Different colors indicate the magnitude of the fluid velocity vector. Right: Dependence of water level on time at points P1-P4.

Next, we simulate a rock landslide on the right-bank slope near the same dam. Due to the absence of the rheological data for the considered slope, we adopted the coefficients K, τ_s, n of the Hershel-Bulkley model from [1] measured for rock landslides in the south of Italy. Figure 3 (left) shows the top view of the landslide at intermediate time moment and the velocities of the fluid. The graph of the maximal pressure acting on the dam structures at the place of landslide is given in figure 3 (right). The maximal number of cells in the computational meshes approached 560 thousand.

Finally, we simulate a tsunami run-up in two stages. At the first stage we solve the shallow water equations [18] for horizontal velocity components and water level defined in the World Ocean. The solution is based on the mixed finite element method [2] on unstructured triangulation of the World Ocean and the fractional time stepping scheme [6]. At the second stage,

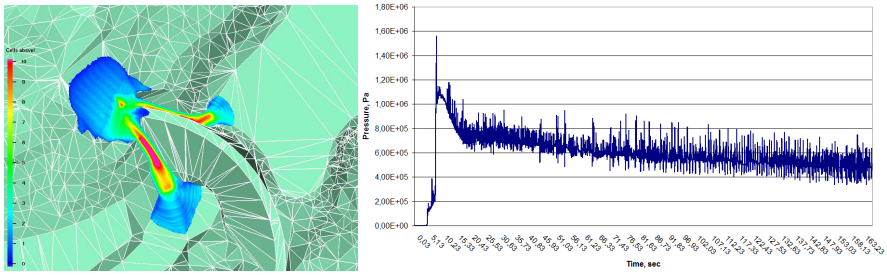

Fig. 3. Left: Migration of the landslide at time moment $t = 100$s. Different colors mark the velocity vector magnitudes for the particles of the landslide. Right: The pressure experienced by the dam at the place of the landslide.

when the tsunami wave approaches the shore, we adopt the elevation and horizontal velocity in the boundary conditions of the 3D free surface flow model presented in section 2. Figure 4 (left) demonstrates the tsunami wave

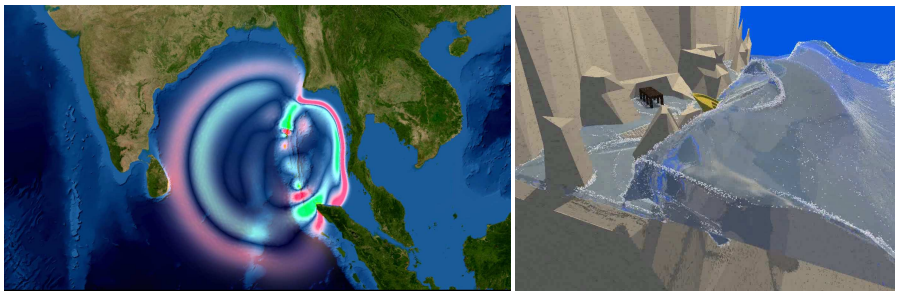

Fig. 4. Left: Tsunami elevation in 100 minutes after an earthquake in the Bay of Bengal. Different colors mark the ocean elevation. Right: tsunami run-up in a bay with rocky relief.

elevation in 100 minutes after a hypothetical earthquake with epicenter at $9°40'$ north latitude and $92°30'$ east longitude. The epicenter is located in seismically active region between Andaman and Nicobar islands in the Bay of Bengal. The colored field of ocean elevation is superposed on the Google Earth images of the Bay of Bengal. The features of tsunami run-up depend on the ocean bed and the terrain. The terrain shown in figure 1 (right) is capable to produce wave breaking, which is dangerous for boats and facilities, see figure 4 (right). Development and breaking of waves in the run-up can be inspected in [19].

This work has been supported in part by RFBR grants 12-01-31233, 12-01-31275, 12-01-33084, 12-01-00283, 12-01-91330, the Russian President grants MK 3675.2013.1, MK 7159.2013.1, Federal programs "Scientific and scientific-pedagogical personnel of innovative Russia", "Research and Development", and Russian Academy of Science project No. 01.2.00104588.

References

1. T. Bisantino, P. Fischer, F. Gentile, *Rheological characteristics of debris-flow material in South-Gargano watersheds*, Nat. Hazards, **54** (2010), 209–223.
2. C. Cotter, D. Ham, C. Pain, *A mixed discontinuous/continuous finite element pair for shallow-water ocean modeling*, Ocean Modelling, **26**, (2009), 86–90.
3. W.H. Herschel, R. Bulkley, *Measurement of consistency as applied to rubber-benzene solutions*, Proc. Am. Assoc. Test Mater. Part II, **26** (1926), 621–629.
4. R.M. Iverson, *The physics of debris flows*, Rev. Geoph., **35** (1997), 245–296.
5. F. Losasso, F. Gibou, R. Fedkiw, *Simulating water and smoke with an octree data structure*, ACM Transactions on Graphics (TOG), **23**:3, August 2004.
6. G.I. Marchuk, A.S. Sarkisyan (Eds.) *Mathematical models of ocean circulation*. Novosibirsk, Nauka, 1980.
7. C. Min, F. Gibou, *A second order accurate level set method on non-graded adaptive cartesian grids*, J. Comput. Phys., **225** (2007), 300–321.
8. K.D. Nikitin, Y.V. Vassilevski, *Free surface flow modelling on dynamically refined hexahedral meshes*, Rus. J. Num. Anal. Math. Model., **23** (2008), 469–485.
9. K.D. Nikitin, M.A. Olshanskii , K.M. Terekhov, Y.V. Vassilevski, *Numerical simulations of free surface flows on adaptive cartesian grids with level set function method*, Preprint is available online, 2010.
10. K.D. Nikitin, M.A. Olshanskii , K.M. Terekhov, Y.V. Vassilevski, *A numerical method for the simulation of free surface flows of viscoplastic fluid in 3D*, J. Comp. Math., **29** (2011), 605–622.
11. M.A. Olshanskii , K.M. Terekhov, Y.V. Vassilevski, *An octree-based solver for the incompressible Navier-Stokes equations with enhanced stability and low dissipation*, Computers & Fluids, **84** (2013), 231–246.
12. S. Osher, R. Fedkiw, *Level Set Methods and Dynamic Implicit Surfaces.* Springer-Verlag, 2002.
13. E.N. Pelinovskii, *Hydrodynamics of Tsunami Waves*, IAP RAS, Nizhn. Novgorod, 1996
14. S. Popinet, *An accurate adaptive solver for surface-tension-driven interfacial flows*, J. Comput. Phys., **228** (2009), 5838–5866.
15. M. Sussman, P. Smereka, S. Osher, *A level set approach for computing solutions to incompressible two-phase flow*, J. Comput. Phys., **114** (1994), 146–159.
16. J. Strain, *Semi-Lagrangian methods for level set equations*, J. Comput. Phys., **151** (1999), 498–533.
17. Y.V. Vassilevski, K.D. Nikitin, M.A. Olshanskii , K.M. Terekhov, *CFD technology for 3D simulation of large-scale hydrodynamic events and disasters*, Rus. J. Numer. Anal. Math. Model., **27** (2012), 399–412.
18. C.B. Vreugdenhil, *Numerical Methods for Shallow-Water Flow*, Kluwer Academic Publishers, 1994.
19. http://dodo.inm.ras.ru/research/freesurface.